COMPUTATIONAL PROBLEMS OF ELECTRICAL ENGINEERING

Vol. 5, No. 2, 2015

RESEARCH INTO AMBIGUITY FUNCTION OF NARROW-BAND, MULTI-BAND AND ULTRA-WIDEBAND RADIOMETRIC COMPLEXES WITH MULTI-ANTENNA SYSTEMS

Nguyen Van Kiem[1], Vladimir Pavlikov[1], Olena Tymoshchuk[2]

[1] N. Ye. Zhukovsky National Aerospace University - Kharkiv Aviation Institute, Kharkiv, Ukraine

[2] Institute of Water Transport, Petro Konashevych-Sahaydachniy State Maritime Academy, Kyiv, Ukraine

kiemxai@gmail.com, pavlikov_kharkov@mail.ru, tymoshchukom@gmail.com

Abstract: An optimal algorithm for radiometric imaging with high spatial resolution is obtained. An analytical expression for the ambiguity function (AF) of narrow-band, multi-band and ultra-wideband (UWB) radiometric complexes with multi-antenna systems is derived. The impact of the antennas geometry, antennas number, as well as the narrow-band, multi-band and UWB predetection section on spatial resolution is investigated. It is shown that using multi-antenna systems with multi-band and UWB signal processing contributes to the formation of AF with one main lobe.

Key words: radiometry, ambiguity function, ultra-wideband radiometric complex.

1. Introduction

Radiometric complexes (RMC) [1–7] are used for radiometric imaging in remote sensing and radio astronomy. These complexes allow the high spatial resolution and sensitivity fluctuation to be obtained. In [8–11], an optimal algorithm for ultra-wideband (UWB) spatio-temporal signal processing with multi-antennas complexes was synthesized, and it was shown that UWB signal processing allows the sensitivity fluctuation of RMC to be essentially improved. The geometry of antenna array, number of antennas in the array and bandwidth of operating frequencies in the predetection section remains unstudied.

Continuing the research described in [12], in the article, the problem of statistical synthesis of an UWB multi-antenna RMC for radiometric imaging with high spatial resolution is solved, and its ambiguity function (AF) is investigated for the different number of antennas in the array, different geometries of antenna arrays (AA) and different frequency bandwidths.

2. Problem statement

It is necessary to synthesize an optimal algorithm for radiometric imaging in multi-antenna RMC, to isolate AF and explore it in terms of the UWB, multi-band and narrow-band predetection section.

Source data define the following model of an observation equation:

$$\underset{\sim}{u}(t)=\{u_i(t)\}_{i=1}^{M}=\{s_i(t)+n_i(t)\}_{i=1}^{M}, \qquad (1)$$

where $s_i(t)$ is the noise radiation of the investigated object after the predetection section of the i^{th} receiver channel, $n_i(t)$ is the internal receiver noise. The processes $s_i(t)$, $n_i(t)$ are the Gaussian non cross-correlated noises with zero-means.

3. Problem solution

Algorithm synthesis. We use the method of maximum likelihood to synthesize an optimal algorithm of radiometric imaging. For this purpose, we shall solve the following equation:

$$-\frac{1}{2}\int_0^{T_{ob}}\int_0^{T_{ob}}\frac{d\,\underline{R}(t_1,t_2,B(f,\underset{\sim}{J}'))}{d\,B(f,\underset{\sim}{J})}\underline{W}(t_2,t_1,B(f,\underset{\sim}{J}'))dt_1dt_2-$$
$$-\frac{1}{2}\int_0^{T_{ob}}\int_0^{T_{ob}}\underset{\sim}{u}^T(t_1)\frac{d\,\underline{W}(t_1,t_2,B(f,\underset{\sim}{J}'))}{d\,B(f,\underset{\sim}{J})}\underset{\sim}{u}(t_2)dt_1dt_2=0, \qquad (2)$$

where T_{ob} denotes the time of observation, $d/d\,B(f,\underset{\sim}{J})$ represents the functional derivative, $B\left(f,\underset{\sim}{J}\right)$ is the spectral angular power density (radio brightness), $\underline{R}\left(t_1,t_2,B(f,\underset{\sim}{J}')\right)$ stands for the correlation matrix of observation processes, $\underline{W}\left(t_1,t_2,B(f,\underset{\sim}{J}')\right)$ is the matrix inverse to the matrix of correlation functions.

In the spectral region, equation (2) takes the form:

$$-T_{ob}Spur\int_{-\infty}^{\infty}\left\{\begin{array}{c}\dfrac{d\,\underline{G}_u\left(f,\underset{\sim}{J}_0,\underline{\Delta a},B(f,\underset{\sim}{J}')\right)}{d\,B(f,\underset{\sim}{J}')}\times\\ \times\left[\underline{G}_u^{-1}\left(f,\underset{\sim}{J}_0,\underline{\Delta a},B(f,\underset{\sim}{J}')\right)\right]^T\end{array}\right\}df=$$
$$=\int_{-\infty}^{\infty}\left\{\begin{array}{c}\underset{\sim}{U}_T^{T*}(j2\pi f)\times\\ \times\dfrac{d\,\underline{G}_u^{-1}\left(f,\underset{\sim}{J}_0,\underline{\Delta a},B(f,\underset{\sim}{J}')\right)}{d\,B(f,\underset{\sim}{J}')}\times\\ \times\underset{\sim}{U}_T(j2\pi f)\end{array}\right\}df \qquad (3)$$

where

$$\underline{\Delta \vec{a}} = \begin{bmatrix} 0 & \vec{a}_1 - \vec{a}_2 & \mathbf{L} & \vec{a}_1 - \vec{a}_M \\ \vec{a}_2 - \vec{a}_1 & 0 & \mathbf{L} & \vec{a}_2 - \vec{a}_M \\ \mathbf{M} & \mathbf{M} & \mathbf{O} & \mathbf{M} \\ \vec{a}_M - \vec{a}_1 & \vec{a}_M - \vec{a}_2 & \mathbf{L} & 0 \end{bmatrix} \quad (4)$$

is the matrix of distance vectors for all pairs of radio interferometers in RMC, *Spur* denotes the trace of matrix, "$*$" represents the sign of the complex conjugation operator, "T" is the sign of the transpose operator, $\hat{U}^{T}(j2\pi f) = \left\| \hat{U}_1(j2\pi f) \quad \mathbf{L} \quad \hat{U}_M(j2\pi f) \right\|$ is the vector of observation spectra,

$$\hat{U}_T(j2\pi f) = \int_0^T u(t) e^{-j2\pi f t} dt, \quad (5)$$

$\underline{I}$ stands for the identity matrix. Here $\underline{G}_u(f,\cdot)$ is the power spectral density (PSD) matrix, which is determined by the Fourier transformation of a correlation function matrix

$$\underline{G}_u(f) = F\{\underline{R}_u(t_1 - t_2)\} = \left\| \begin{matrix} 0 & \hat{G}_{s12} & \mathbf{K} & \hat{G}_{s1M} \\ \hat{G}_{s21} & 0 & \mathbf{L} & \hat{G}_{s2M} \\ \mathbf{M} & \mathbf{M} & \mathbf{O} & \mathbf{M} \\ \hat{G}_{sM1} & \hat{G}_{sM2} & \mathbf{L} & 0 \end{matrix} \right\|, \quad (6)$$

$$G_{sij} = 0,5 \left| \hat{K}(j2\pi f) \right|^2 \int_{-\infty}^{\infty} A_{eff}(f, \vec{J} - \vec{J}_0) \times \times B(f, \vec{J}) \exp(j2\pi f \Delta \vec{a}_{ij} (\vec{J} - \vec{J}_0) c^{-1}) d\vec{J} = \quad (7)$$
$$= 0,5 \left| \hat{K} \right|^2 B_{Aij}, i, j = 1..M, i \neq j.$$

Here $A_{eff}(f, \vec{J} - \vec{J}_0)$ is the aperture area (effective antenna area), $\hat{K}(j2\pi f)$ represents the transfer characteristic of the predetection section of each channel, $\vec{J}$ denotes the vector of direction cosines, $\vec{J}_0$ is the vector of direction cosines for the direction of the main beam of an antenna pattern, f stands for the frequency, $\Delta \vec{a}_{ij} = \vec{a}_i - \vec{a}_j$, $\vec{a}_i$ are the base between the i[th] and j[th] antennas, c is the radiowave propagation speed. In (3), $\underline{G}_u^{-1}\left(f, \vec{J}_0, \underline{\Delta \vec{a}}, B(f, \vec{J})\right)$ is the inverse PSD matrix, which is determined from the equation below.

$$\underline{G}_u\left(f, \vec{J}_0, \underline{\Delta \vec{a}}, B(f, \vec{J})\right) \times \times \underline{G}_u^{-1}\left(f, \vec{J}_0, \underline{\Delta \vec{a}}, B(f, \vec{J})\right) = \underline{I}. \quad (8)$$

Solution (3) takes the following form:

$$\int_{-\infty}^{\infty} \left\{ A_{eff}(f, \vec{J} - \vec{J}_0) \left| \hat{K}(j2\pi f) \right|^2 \times \times \sum_{\substack{i,j=1 \\ i \neq j}}^{M} Q_{ij} e^{j2\pi f (\vec{J} - \vec{J}_0) \Delta \vec{a}_{ij} c^{-1}} \right\} df =$$
$$= T_{ob}^{-1} \int_{-\infty}^{\infty} A_{eff}(f, \vec{J} - \vec{J}_0) \left| \hat{K}(j2\pi f) \right|^2 \times \quad (9)$$
$$\times \sum_{\substack{i,j=1 \\ i \neq j}}^{M} \hat{U}_{T,i}(j2\pi f) \hat{U}^{*}_{T,j}(j2\pi f) Q_{ji}^2 e^{j2\pi f (\vec{J} - \vec{J}_0) \Delta \vec{a}_{ij} c^{-1}} df,$$

where Q_{ij} is the element of the matrix $\underline{G}_u^{-1}(\cdot)$.

AF of RMC. An ambiguity function is a response of the system to the point source of radio emission [8] $B(f, \vec{J}) = d(\vec{J} - \vec{J}_0')$. Then we substitute $d(\vec{J} - \vec{J}_0')$ for the left side of (9) and obtain the following AF:

$$\Psi(\cdot) = \frac{2}{(M-1)} \int_{-\infty}^{\infty} \left\{ A_{eff,N}(f, \vec{J} - \vec{J}_0) \times \times \sum_{\substack{i,j=1 \\ i \neq j}}^{M} e^{j2\pi f (\vec{J} - \vec{J}_0 + \vec{J}_0' - \vec{J}_0) \Delta \vec{a}_{ij} c^{-1}} \right\} df, \quad (10)$$

where $A_{eff,N}(f, \vec{J} - \vec{J}_0) = \dfrac{A_{eff}(f, \vec{J} - \vec{J}_0)}{A_{eff}(f, \vec{J}_0' - \vec{J}_0)}$ is the normalized aperture area (effective antenna area).

As follows from the analysis of (10), AF depends on the geometry of antenna system, radiation pattern of a single antenna, the number of antennas in the array and operating frequency range.

We shall analyze the impact of the AA geometry, the antennas number and bandwidth on the properties of AF. Simultaneously with the AF analysis, we shall give the regions of spatio-spectral sensitivity (SSS), which are commonly used in radio astronomy problems.

AF and functions of SSS of narrow-band multi-antenna RMC. Let us consider AA with the antennas number 5×5 (Fig. 1.a) and 7×7 (Fig. 2.a) elements. The dimensions of AA are the same, the central frequency is $f_0 = 1,4$ GHz, the bandwidth is $\Delta f = 1$ KHz.

As follows from the analysis of Fig. 1 and Fig. 2, with the density of antennas in a narrow-band AA increasing, the ambiguity of coordination measurements decreases. In the boundary case, when AA is densely filled, AF have a near continual aperture of the same size. In RMC, an increase in the density of antennas in AA is reached by the methods of parallel or serial synthesis. The former is associated with the filling (appreciation) of RMC, the latter increases the time of measurement. To reduce the numbers of antennas in the systems of parallel type and time of observation in the systems of serial type, it is expedient to use the multi-band RMC, which we shall consider in the next paragraph.

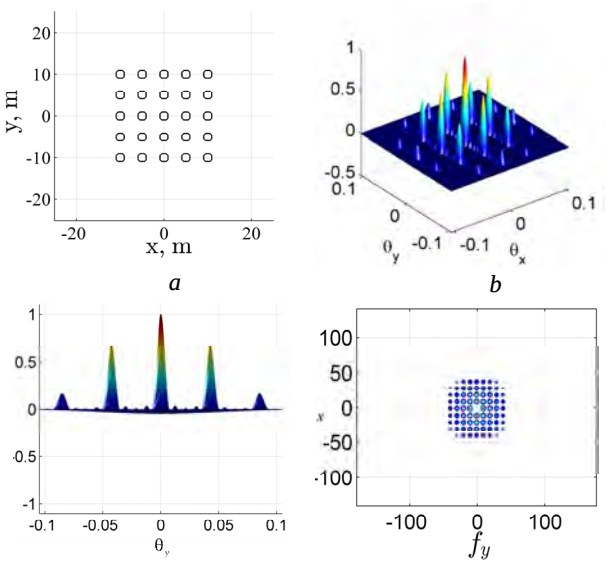

Fig. 1. AA with 5×5 *elements (a), AF of RMC (b), projection of AF on the plane* q_y0z *(c), SSS region (d).*

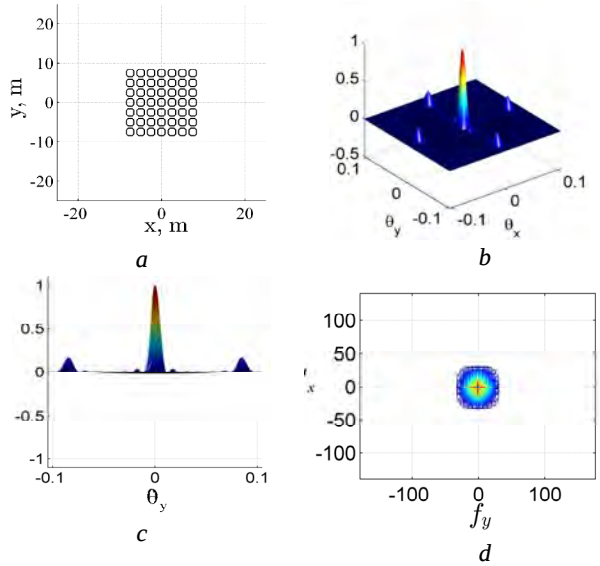

Fig. 2. AA with 7×7 *elements (a), AF of RMC (b), projection of AF on the plane* q_y0z *(c), SSS region (d).*

AF of multi-band RMC. Let there be a 25-element AA (5×5 elements, see Fig. 1.a). Let us assume that each antenna delivers signals at the frequencies of [1,4–1,8] GHz and [2,2–2,6] GHz. The AF and SSS region of such a system are shown in Fig. 3. In Fig. 4, the AF and SSS region are shown for the frequencies of [1,4–1,8] GHz, [2,2–2,6] GHz and [2,8–3,5] GHz.

As follows from the analysis of Fig. 3 and Fig. 4, signal processing in several frequency bands reduces the level of AF side lobes and provides the filling of the SSS region. In other words, it is advisable to use the wideband and ultra-wideband signal processing.

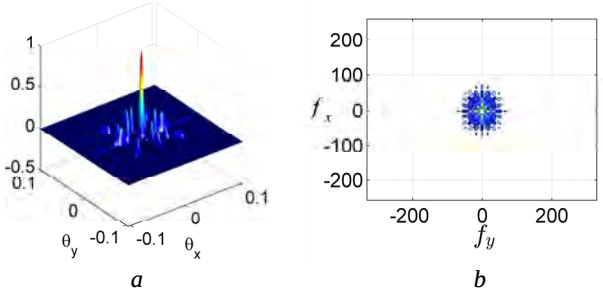

Fig. 3. AF of RMC with 5×5 *- element AA (two bands) (a), SSS region (b).*

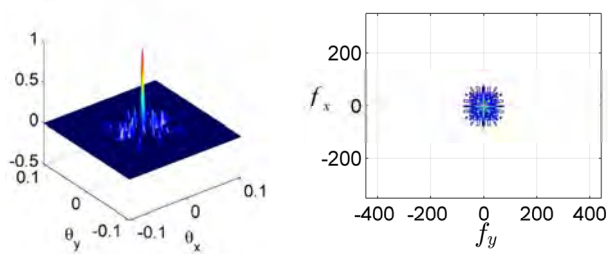

Fig. 4. AF of RMC with 5×5 *- element AA (three bands) (a), SSS region (b).*

AF of UWB RMC. Again, we assume that there is a 25-element AA (5×5 elements, see Fig. 1.a). Let us assume that each antenna transmits signals at the frequencies of [1,4–3,5] GHz. Fig. 5 shows the AF and SSS region of such a system.

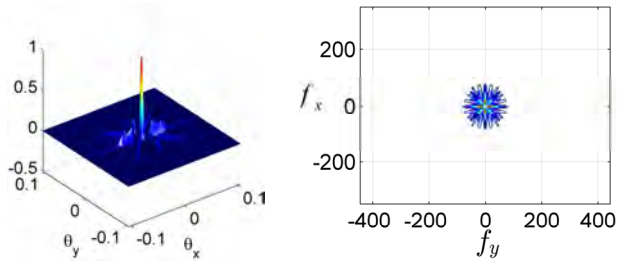

Fig. 5. AF of UWB RMC with a 5×5 *- element AA (a), SSS region (b).*

As follows from the analysis of Fig. 5, using UWB RMC reduces significantly the ambiguity of measurement of radiometric images and fills a SSS region or, what is the same, synthesizes the aperture in the spatial frequency plane.

Investigation of the possibility of reducing the number of antennas in AA of UWB RMC. Research into AF of RMC with ultra sparse AA. For the advantages of UWB systems to be used effectively, it is necessary to study the geometry of AA. The question of the AA optimization is quite complicated and goes beyond the bounds of the article. Next, we analyze AF with X-shaped, Y-shaped, spiral and circular AA.

The X-shaped AA. The geometry of an X-shaped AA is shown in Fig. 6. a. The AF and SSS region

for quasi-monochromatic ($f_0 = 1{,}4$ GHz), three-band ([1,4–1,8], [2,2–2,6] and [2,8–3,5] GHz) and ultra-wideband (UWB) ([1,4–3,5] GHz.) RMC are shown in Fig. 7 and Fig. 8.

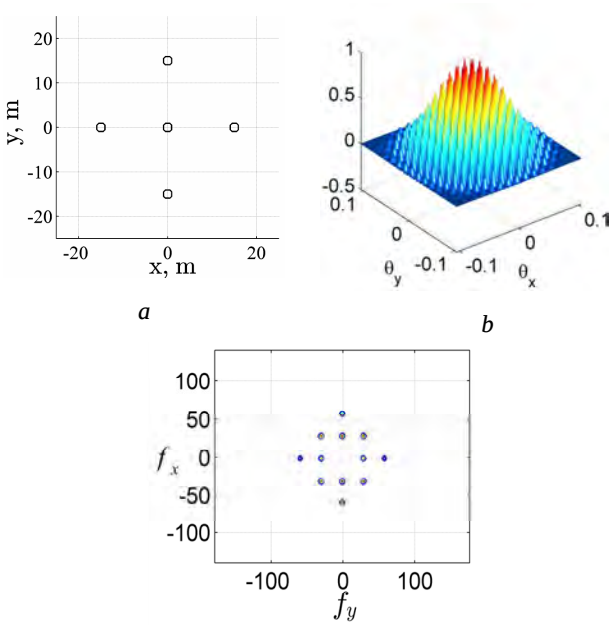

Fig. 6. X-shaped AA (a), AF (b), SSS region of quasi-monochromatic RMC (c).

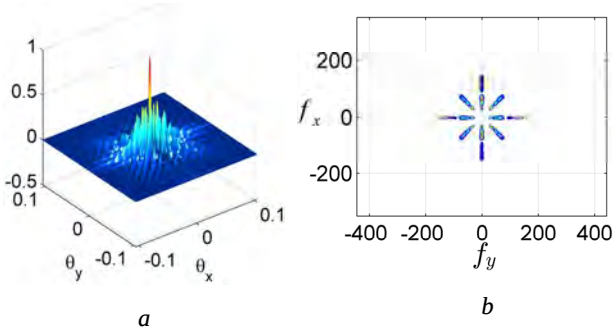

Fig. 7. AF with an X-shaped AA (a), SSS region of a three-band RMC (b).

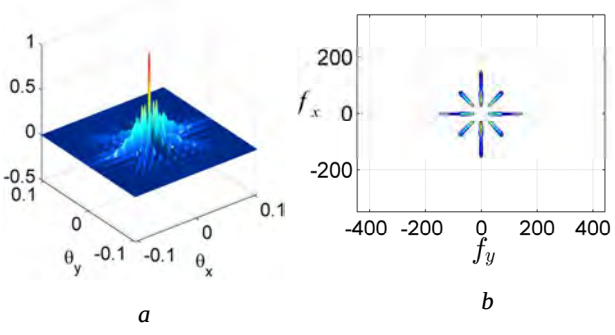

Fig. 8. AF of RMC with an X-shaped AA (a), SSS region of UWB RMC (b).

The Y-shaped AA. The geometry of a Y-shaped AA is shown in Fig. 9.a. The AF and SSS region for quasi-monochromatic, three-band and ultra-wideband RMC are shown in Fig. 9–11.

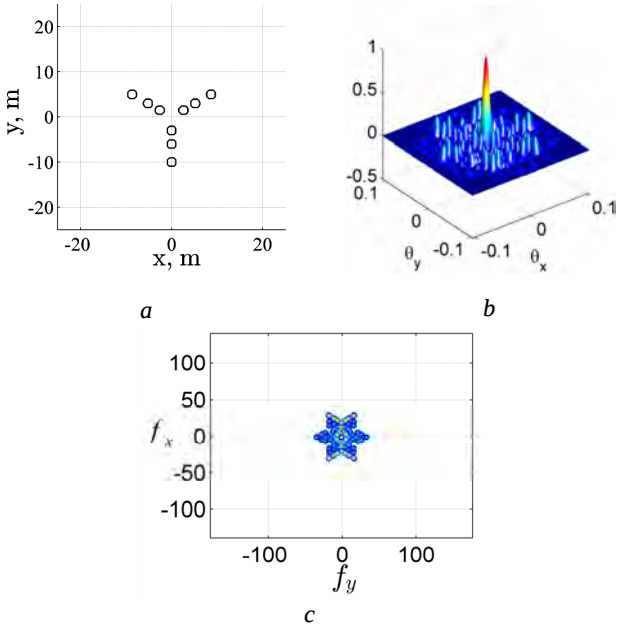

Fig. 9. Y-shaped AA (a), AF (b), SSS region of quasi-monochromatic RMC (c).

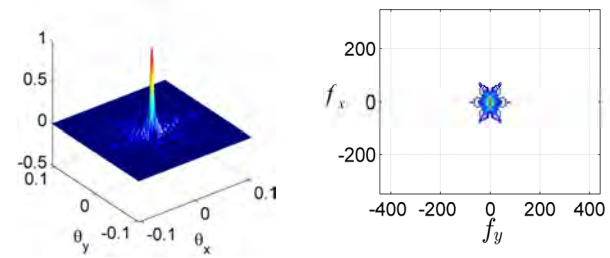

Fig. 10. AF of an Y-shaped AA (a), SSS region of a three- band RMC (b).

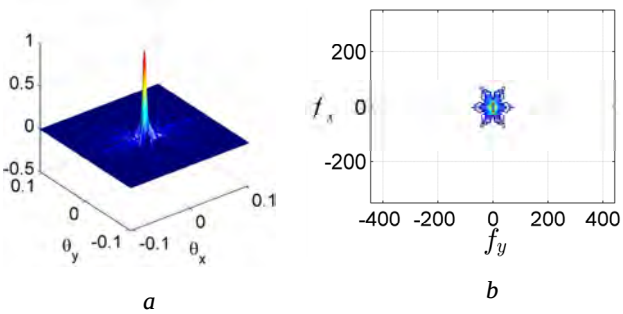

Fig. 11. AF of an Y-shaped AA (a), SSS region of UWB RMC (b).

The spiral-shaped AA. The geometry of a spiral-shaped AA is shown in Fig. 12.a. AF and SSS region for

quasimonochromatic, three-band and UWB RMC are shown in Fig. 12–14.

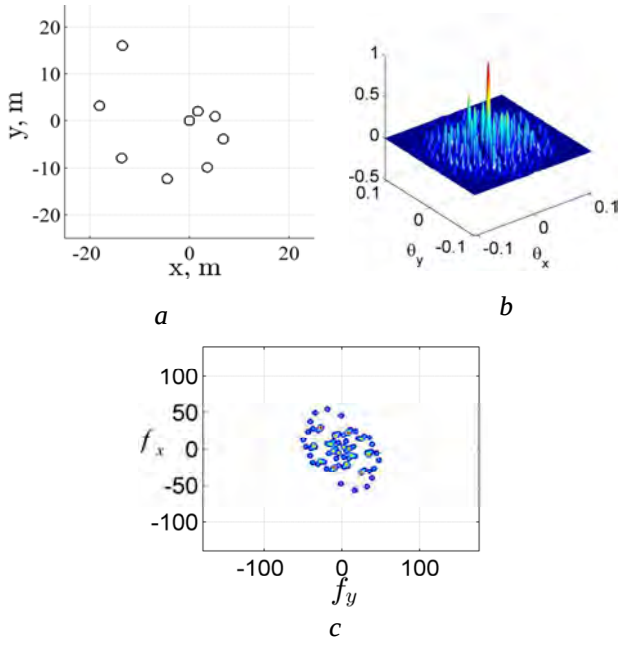

Fig. 12. Spiral-shaped AA (a), AF (b), SSS region of quasi-monochromatic RMC (c).

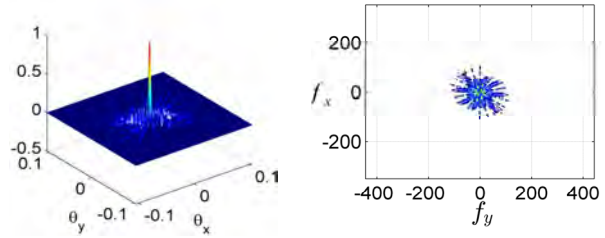

Fig. 13. AF (a), SSS region of a three-band RMC (b).

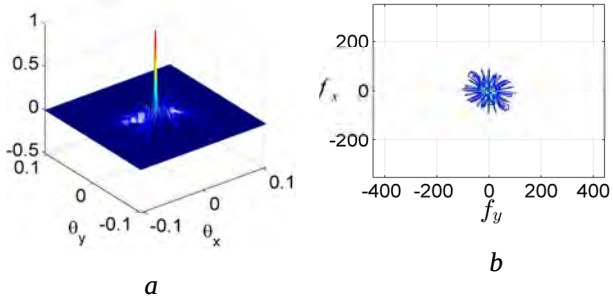

Fig. 14. AF of a spiral-shaped AA (a), SSS region of UWB RMC (b).

The circular-shaped AA. The geometry of a circular-shaped AA is shown in Fig. 15.a. AF and SSS region for quasimonochromatic, three-band and UWB RMC are shown in Fig. 15–17.

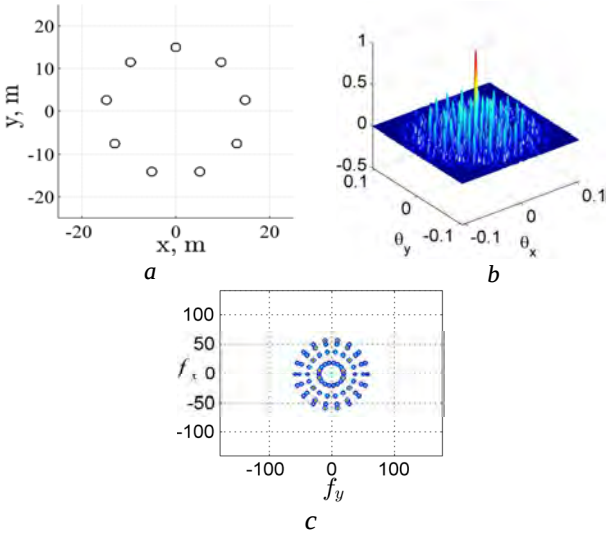

Fig. 15. Circular-shaped AA (a), AF (b), SSS region of quasi-monochromatic RMC (c).

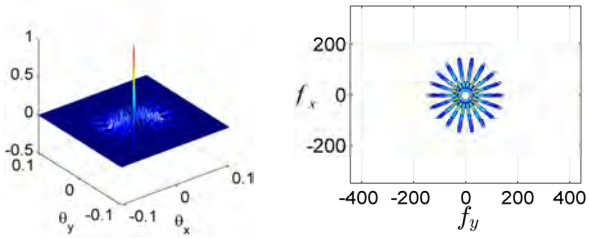

Fig. 16. AF (a), SSS region of a three-band RMC (b).

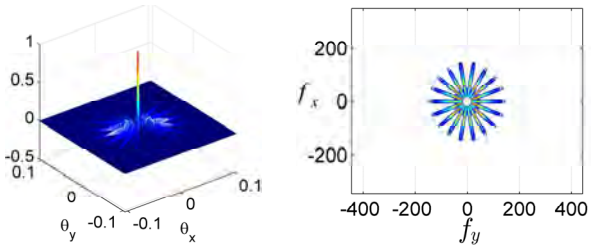

Fig. 17. AF of a circular-shaped (a), SSS region of UWB RMC (b).

The analysis of AF of RMC has resulted in the following conclusions:

- transition to ultra sparse AA is expedient with the joint use of multi-band or UWB RMC. Using UWB of the predetection section excludes multilobes of AF of RMC;
- the use of a small number of antennas in AA, which are arranged in such a way to exclude redundant bases (of the same size and direction) and ensure the greatest possible number of independent directions has its prospects. The side lode level in multi-antenna RMC depends on the number of antennas, the size and orientation of the base of different antenna pairs in AA. The smallest side lobe level is achieved by using circular AA and UWB RMC.

4. Conclusions

An analytical expression for the ambiguity function of radiometric complexes with multi-antenna system has been derived. The ambiguity functions of narrow-band, multi-band and UWB RMC for various geometries of AA have been investigated. The expediency of using multi-band and UWB RMC with ultra sparse AA has been substantiated. It has been shown that using UWB RMC contributes to achieving the following important results: a small number of antennas in RMC of parallel type and short time of observation in RMC of series type. The former allows a significant reduction in the cost of system design, and the latter is important for the investigation of sources with rapid fluctuations of the statistical characteristic.

References

[1] A. Grigoriev, "Method of radiometric distortion correction of multispectral data for the earth remote sensing". *Scientific. and Tech. Journal of Information Technologies, Mechanics and Optics*, vol. 15, no. 4, pp. 595–602, 2015.

[2] P. Goldsmith, "Instrumentation and Techniques for Radio Astronomy", *IEEE Press: New York*, (Ed) 1988.

[3] B. Burke and Graham-Smith, "An Introduction to Radio Astronomy", *Cambridge University Press*, 1997.

[4] Y. Kerr, et al., "The SMOS Soil Moisture Retrieval Algorithm", *IEEE Transactions on Geoscience and Remote Sensing*, vol. 50, no. 5, pp. 1384–1403, 2012.

[5] J. Pasachoff and A. Filippenko, "The Cosmos: Astronomy in the New Millennium", 4th ed. 2013.

[6] V. Volosyuk and V.Kravchenko, *Statistical Theory of Radio-Engineering Systems of Remote Sensing and Radar*, Fizmatlit, Moscow, 2008. (Russian)

[7] V. Volosyuk, V. Kravchenko, and V. Pavlikov, "Development of the theory, methods and algorithms for optimal wide- and ultrawideband spatiotemporal signal processing of radio-thermal radiation", in *Proc. IX Intern. conf. ICATT'2013*, pp. 74−79, Ukraine, 2013.

[8] V. Pavlikov, S. Zhyla, Nguyen Van Kiem and O. V. Odokienko, 'Optimal signal processing for radiometric imaging with multi-antenna & multi-band passive radars", in *Proc. X Intern. conf. ICATT'2015. Antenna theory and techniques*, pp. 179–181, Kharkiv, Ukraine, Apr. 2015.

[9] N. Kiem and O. Tymoshchuk, "Investigation of ambiguity function of ultra-wideband, multi-band and narrow-band radiometric complex with a three-element-antenna system". in *Proc. XIII Intern. Conf. TCSET'2016*, pp. 240–242, Lviv-Slavske, Ukraine, 2016.

[10] N.Kiem and O.Tymoshchuk, "Radiobrightness optimal estimation of extended sources of radio thermal radiation in two antenna ultra-wideband radiometric system", *Radioelectr. and computer system*, vol. 74, no. 4, pp. 13–18, 2015. (Russian)

[11] V. Pavlikov, N.Kiem, and O.Tymoshchuk, "Synthesis of optimal estimation algorithm of radiometric images in ultra-wideband radiometric complex with three-element antenna system", *Aviation and space technology*, vol. 123, no. 6, pp. 64–68, 2015. (Russian)

[12] V. Pavlikov, N. Kiem, and O. Tymoshchuk, "Optimal Structural Synthesis of Multi-Antenna Ultra-Wideband Radiometric Complex", in *Proc. 9th Intern. Symp. on Physics and Eng. of Microwaves MSMW'2016, Ukraine.*

ДОСЛІДЖЕННЯ ФУНКЦІЇ НЕВИЗНАЧЕНОСТІ ВУЗЬКОСМУГОВИХ, БАГАТОСМУГОВИХ І НАДШИРОКОСМУГОВИХ РАДІОМЕТРИЧНИХ КОМПЛЕКСІВ З БАГАТОАНТЕННИМИ СИСТЕМАМИ

Нгуєн Ван Кіем, Владімір Павліков, Олена Тимощук

Отримано оптимальний алгоритм для формування радіометричних зображень з високим просторовим розрізненням. Виведено аналітичний вираз для функції невизначеності (ФН) вузькосмугових, багатосмугових і надширокосмугових (НШС) радіометричних комплексів з багатоантенними системами. Досліджено залежність геометрії розташування антен, кількість антен і використання вузькосмугового, багатосмугового і НШС вхідних трактів на вигляд ФН. Показано, що використання багатоантенних систем з обробкою НШС і багатосмугових сигналів дає змогу сформувати ФН з однією головною пелюсткою.

Nguyen Van Kiem, Ph. D. student at Department of Design of Radio Engineering Systems of Aircraft, N. Ye. Zhukovsky National Aerospace University – Kharkiv Aviation Institute, Ukraine.

Vladimir Pavlikov, Doctor of Technical Sciences, Senior Researcher, Head of Department of Design of Radio Engineering Systems of Aircraft, N. Ye. Zhukovsky National Aerospace University – Kharkiv Aviation Institute, Ukraine.

Olena Tymoshchuk, Director of the Institute of Water Transport, Petro Konashevych-Sahaydachniy State Maritime Academy, Kyiv, Ukraine.